HHS Public Access

Author manuscript

Glia. Author manuscript; available in PMC 2016 October 01.

Published in final edited form as:

Glia. 2015 October ; 63(10): 1694–1713. doi:10.1002/glia.22835.

Transient activation of microglia following acute alcohol exposure in developing mouse neocortex is primarily driven by BAX-dependent neurodegeneration

Katelin E. Ahlers[1], **Bahri Karaçay**[2], **Leah Fuller**[1], **Daniel J. Bonthius**[2,3], and **Michael E. Dailey**[1]

[1]Department of Biology, College of Liberal Arts and Sciences, University of Iowa, Iowa City, IA 52242

[2]Division of Child Neurology, Department of Pediatrics, The Roy J. Carver College of Medicine, University of Iowa, Iowa City, IA 52242

[3]Department of Neurology, The Roy J. Carver College of Medicine, University of Iowa, Iowa City, IA 52242

Abstract

Fetal alcohol exposure is the most common known cause of preventable mental retardation, yet we know little about how microglia respond to, or are affected by, alcohol in the developing brain *in vivo*. Using an acute (single day) model of moderate (3 g/kg) to severe (5 g/kg) alcohol exposure in postnatal day (P) 7 or P8 mice, we found that alcohol-induced neuroapoptosis in the neocortex is closely correlated in space and time with the appearance of activated microglia near dead cells. The timing and molecular pattern of microglial activation varied with the level of cell death. Although microglia rapidly mobilized to contact and engulf late stage apoptotic neurons, apoptotic bodies temporarily accumulated in neocortex, suggesting that in severe cases of alcohol toxicity the neurodegeneration rate exceeds the clearance capacity of endogenous microglia. Nevertheless, most dead cells were cleared and microglia began to deactivate within 1-2 days of the initial insult. Coincident with microglial activation and deactivation, there was a transient increase in expression of pro-inflammatory factors, TNFα and IL-1β, after severe (5 g/kg) but not moderate (3 g/kg) EtOH levels. Alcohol-induced microglial activation and pro-inflammatory factor expression were largely abolished in BAX null mice lacking neuroapoptosis, indicating that microglial activation is primarily triggered by apoptosis rather than the alcohol. Therefore, acute alcohol exposure in the developing neocortex causes transient microglial activation and mobilization, promoting clearance of dead cells and tissue recovery. Moreover, cortical microglia show a remarkable capacity to rapidly deactivate following even severe neurodegenerative insults in the developing brain.

Keywords

development; apoptosis; phagocytosis; fetal alcohol spectrum disorders

Correspondence to: Dr. Michael E. Dailey, Dept. of Biology, 369 Biology Building, University of Iowa, Iowa City, IA 52242-1324, Michael-e-dailey@uiowa.edu, TEL: (319) 335-1067.

The authors declare that they have no conflict of interest.

Introduction

Microglial responses to neuronal injury or neurodegenerative conditions in the mature and aging brain are being studied extensively (Eggen et al., 2013), but comparatively little is known regarding microglial responses to neuronal injury in the developing brain. Since microglia in the developing brain are immature (Harry, 2013), they may react to neuronal injury very differently than their counterparts in the mature or aging brain. To study microglial responses to neuronal injury in the developing brain, we used a modified neonatal mouse model of acute alcohol exposure (Bonthius et al., 2002) that induces apoptotic neurodegeneration in the cerebral cortex (Bonthius et al., 2002; Olney et al., 2002) and thereby mimics severe Fetal Alcohol Spectrum Disorders (FASDs).

Fetal alcohol exposure is the most common known cause of preventable mental retardation in humans, potentially affecting 2-5% of children (May et al., 2009). Severe alcohol exposure *in utero* leads to neurodegeneration and reduced brain volume in humans (Chen et al., 2003). In mouse models, even a single binge-like alcohol exposure during critical periods of brain development induces widespread apoptotic neurodegeneration and cognitive deficits (Olney et al., 2002; Sadrian et al., 2012; Saito et al., 2007a,b, 2010; Subbanna et al., 2013; Wilson et al., 2011; Wozniak et al., 2004). Although alcohol's effects on neurons are well studied, much less is known about the effects of alcohol on the structure and function of glia *in situ*, especially microglia in the developing brain (Drew and Kane, 2014; Guizzetti et al., 2014). As brain-resident immune cells, microglia may play either neuroprotective or cytotoxic roles, depending on the context (Aguzzi et al., 2013; Chastain and Sarkar, 2014). Microglia are considered crucial for efficient dead cell clearance, thereby restraining neuroinflammation, limiting secondary damage, and promoting tissue homeostasis (Napoli and Neumann, 2009). Indeed, there is evidence that microglia participate in dead cell clearance after fetal alcohol exposure *in situ* based on colocalization of Iba-1 and phosphorylated tau protein in the cingulate cortex (Saito et al., 2010). However, some cell culture studies have indicated that chronic alcohol exposure inhibits microglial phagocytosis (Aroor and Baker, 1998) and induces microglial expression of pro-inflammatory factors (Boyadjieva and Sarkar, 2010; Fernandez-Lizarbe et al., 2013), which may exacerbate neurodegeneration. In neonatal (P7-P9) rats, 3 days of high (5 g/kg/d or more) alcohol exposure causes elevated expression of pro-inflammatory factors (TNFα and IL-1β) and reactive oxygen species as well as memory impairment in Morris water maze when assessed three weeks later (Marino et al., 2004; Tiwari and Chopra, 2011). Likewise, in adult rat, a 4 day alcohol exposure causes microglial activation and induces expression of proinflammatory cytokines and oxidative enzymes (Crews et al., 2006). As microglia themselves may be vulnerable to alcohol-induced neuroinflammation (Kane et al., 2011), microglial functions during tissue recovery after alcohol exposure may be impaired. Together, these observations have contributed to the notion that alcohol exposure may inhibit microglial phagocytosis, induce a chronically activated pro-inflammatory state, and even kill microglia (Kane et al., 2012). Yet, we do not have a clear understanding of how microglia respond to different levels of alcohol and neuronal injury in the developing brain.

Here we used neonatal GFP-reporter mice to study microglial responses to acute (one day) alcohol exposure in the developing mouse neocortex *in situ*. A single day of alcohol exposure in neonatal rodent is known to induce widespread apoptotic neurodegeneration and cognitive deficits (Olney et al., 2002; Sadrian et al., 2012; Saito et al., 2010; Subbanna et al., 2013; Wilson et al., 2011; Wozniak et al., 2004). Two different concentrations of alcohol (3 and 5 g/kg) were used here in order to determine how microglia respond to differing levels of alcohol and neurodegeneration. We addressed several fundamental questions regarding microglial responses *in situ*: What are the spatial and temporal patterns of microglial activation and inflammation following acute alcohol exposure in developing cerebral cortex? What factors drive microglial activation and inflammation, and how long do microglia remain activated? Do alcohol levels sufficient to kill neurons also kill microglia? To what extent do microglia retain phagocytic ability and contribute to dead cell clearance after alcohol exposure? The results indicate that developing microglia *in vivo* are highly resistant to alcohol's effects and show a remarkably rapid activation and deactivation that is linked to neurodegeneration and clearance of dead cells, thereby promoting homeostasis after injury in the developing cortex.

Materials and Methods

Ethanol Injection and Tissue Harvesting

Postnatal day (P) 7 or P8 C57Bl/6 mouse pups (breeders from Jackson and Harlan Labs) were injected intraperitoneally (IP) (Bonthius et al., 2002) with ethanol (EtOH) at a final concentration of 3 or 5 g/kg. EtOH was delivered as a 20% solution in sterile phosphate buffered saline (PBS) by two injections of 1.5 or 2.5 g/kg EtOH spaced two hours apart. These injections resulted in blood alcohol concentrations (BACs) of ~217 (3 g/kg) and 499 mg/dl (5 g/kg) at 4 h following the first injection (EnzyChromTM Ethanol Assay Kit; BioAssay Systems ECET-100). Control littermates were injected with PBS following the same timeline and volume parameters. Injected pups were returned to their cage with the dam after injection. Pups were weighed before each injection and before sacrifice. To harvest tissues, pups were sacrificed via swift decapitation at 4, 6, 12, 24, 48, or 96 h following the first injection. To maximize the sample size, both males and females were used with equal distribution across experiments. We did not detect any systematic differences between males and females for any of the parameters examined. All animal procedures were performed following guidelines approved by the institutional animal care and use committee.

Mouse lines

For all immunohistochemistry (IHC) experiments, heterozygous GFP-reporter mice [$CX3CR1^{GFP/+}$ (Jung et al., 2000); Jackson Laboratories] in which GFP expression was driven by the fractalkine receptor (CX3CR1) promoter were used so that the fine morphology of microglia could be viewed in combination with multiple fluorescent probes and antibodies. In some experiments, Bcl-2-associated X Protein (BAX)-deficient mice [B6.129X1-Baxtm1Sjk/J; (Knudson et al., 1995); Jackson Laboratories] were crossed with GFP-knock-in ($CX3CR1^{GFP/GFP}$) mice to generate littermates that have GFP-expressing microglia ($CX3CR1^{GFP/+}$) and that are either wild type (BAX WT) or null (BAX KO) for

BAX. All real-time quantitative PCR (RT-qPCR) analyses were performed with WT mice, except for BAX experiments in which heterozygous GFP reporter mice were used. All mouse lines are present on the C57Bl/6 genetic background.

Immunohistochemistry

For IHC, coronal sections of the neocortex were cut (350 μm thick) using a manual tissue chopper, and sections were collected in sequence, rostral to caudal, through the cortex. As they were collected, each section was placed into cold 4 % paraformaldehyde (PFA) in PBS and post-fixed for 24 h at 4°C. After fixation, tissues were washed in PBS, and sections 3-4 mm from the rostral tip of the brain, corresponding to the somatosensory cortex, were processed for IHC. Tissues were de-fatted in 70% EtOH, serially rehydrated, and placed in a blocking/extraction solution [2.5% Normal Goat Serum (Sigma-Aldrich, G9023) and 0.5% Triton®-X-100 in PBS]. After blocking, tissues were incubated for 3 days at 4 °C in rabbit anti-mouse cleaved caspase-3 (CC3; 1:200; Cell Signaling 9661), rat anti-mouse CD68 (1:2000; ED1 clone, AbD Serotec MCA1957), rabbit anti-mouse P2Y12 (1:1000; gift of D. Julius, UCSF), or rat anti-mouse β2/CD18 integrin (1:2000; AbD Serotec MCA1032G) primary antibody diluted in the blocking/extraction solution. Alexa Fluor-647-conjugated goat anti-rabbit or goat anti-rat antibodies (Invitrogen A-21245 and A-21247) were used at a 1:500 dilution in blocking/extraction solution overnight. Lastly, tissues were stained with a fluorescent phosphatidylserine (PS)-binding dye, PSVue-550 (Molecular Targeting Technologies, Inc., MTTI; 1:500) in PBS for 2 h at room temperature, then washed with PBS. PSVue binds at the same epitope on apoptotic cells as annexins but provides a superior signal due to much smaller size of probe and greater concentration of fluorophore.

Confocal Imaging

Fluorescently-stained tissue slices were imaged using a Leica SP5 scanning laser confocal microscope, and the probes were excited using the indicated laser lines: GFP (Argon 488 nm), PSVue-550 (HeNe 543 nm), and Alexa Fluor-647-conjugated secondary antibodies (HeNe 633 nm). To improve the light collection and signal-to-noise ratio, the confocal pinhole was opened to two airy disc units. To capture a large field of view (1,550 × 1,550 μm), stacks of images were collected using a 10×/0.7 Plan Apo objective lens at a xy resolution of 1.3 pixels/μm and with 5 μm z-step intervals. For higher axial resolution of finer structures, a 775 × 775 μm field of view was imaged using a 20×/0.7 Plan Apo objective lens at a xy resolution of 1.4 pixels/μm and with 2 μm z-step intervals. Multi-channel images were combined in ImageJ (Wayne Rasband, NIH). Projection images were made by combining through-focus stacks of images using a maximum brightness operation.

Dead Cell Counts

Quantification of apoptotic cell death was performed by computer-assisted particle analysis of CC3- and PSVue-stained structures in confocal image stacks using ImageJ macros. Analyses were performed in a defined area of interest (AOI) in the dorsal neocortex, just lateral to the cingulate gyrus corresponding to cortical layer IV, a region of high cell death (Fig. 1D and 2D). AOIs were positioned identically in control (PBS) and experimental (EtOH) tissues, and analyses of CC3 and PSVue were performed in separate channels of double-labeled tissues. To facilitate automated particle analysis, color channels were split,

confocal images were processed by background subtraction (rolling ball average), despeckled, and thresholded using a Bernsen autolocal threshold function. Automated counts of particles were performed in each optical section of a z-stack, and the optical section with the highest count was used to represent the AOI. To account for differences in the sizes of early (CC3+)- and later (PSVue+)-stage apoptotic cells, particle size detection ranges were set to 30-500 μm^2 (~6-25 μm diameter) for CC3 and 3-500 μm^2 (~2-25 μm diameter) for PSVue. Analyses were performed for 4-17 fields of view per condition. All results are reported as mean ± standard deviation of the population (SDP). Statistical significance was assessed using two-tailed t-tests. Bonferroni correction for multiple hypotheses was conducted using a family size of four, based on the comparison between PBS- and EtOH-injected animals at each of four time-points. P values ≤ 0.05 were considered significant.

Microglia Cell Density Analysis

Quantification of microglia was performed by particle analysis of GFP-expressing microglia in confocal image stacks using ImageJ macros. These analyses were done blind with respect to the hypothesis that microglial cell number was unaltered at 96 h following alcohol or PBS injection. For consistency, analyses were performed in the same defined AOI as described for the dead cell count analysis described above. To facilitate automated particle analysis, color channels were split, and the GFP confocal channel was despeckled, and thresholded using a Bernsen autolocal threshold function. Automated counts of microglial cell bodies were performed in each optical section of a z-stack, and the optical section with the highest count was used to represent the AOI. To limit counts to only microglial cell bodies and not their branches, particle size detection ranges were set to 50-200 μm^2 with a circularity threshold of 0.3-1. Analyses were performed on 8-10 fields of view per condition. Results are reported as mean ± standard error of the mean (SEM). Statistical significance was assessed using a two-tailed t-test. A p value of ≤ 0.05 was considered significant.

Western blot analysis

For western blot analyses, whole cortical tissues were isolated and placed in brain lysis buffer (150mM NaCl, 1% Triton®-X-100, 10% glycerol, 50mM Tris, pH7.4) with a cOmplete Mini, EDTA-free protease inhibitor cocktail tablet (Roche 11836170001). Tissue and buffer were homogenized using a dounce homogenizer, and centrifuged at 1000g for 15 min (4°C) to isolate the protein-rich supernatant. This supernatant was combined with laemmli buffer and boiled for 5 minutes. Western blots were probed with rabbit anti-mouse CC3 primary antibody (1:200; Cell Signaling 9661) and HRP-linked goat anti-rabbit IgG secondary antibody (1:1000; Cell Signaling 7074). For an internal control, the Western blot was probed with mouse monoclonal β-tubulin primary antibody (1:10,000; Sigma T4026) and HRP-linked goat anti-mouse IgG secondary antibody (1:1000; Merck Millipore DC08L). Antibodies were visualized using the Thermo Scientific™ Super Signal™ West Pico Chemiluminescent Substrate (PI-34078). Film was developed using the Protec ECOMAX X-ray film processor.

Gene Expression Analysis

For RT-qPCR analyses, total RNA was isolated from whole cortical tissues using the TRIzol® reagent (Life Technologies, Gaithersburg, MD) following the manufacturer's instructions. The quantity and quality of RNA were assessed using a NanoDrop 1000 (Thermo Scientific). Total RNA (2 μg) was reverse-transcribed using Superscript^{TM} II (Invitrogen). The resulting cDNA was then diluted 15-fold with RNase-free water. TaqMan® primer and FAM-labeled probe sets for the P2Y12 purinergic receptor (P2Y12, Mm00446026_m1), β2 integrin (Itgβ2, Mm00434523_g1), tumor necrosis factor alpha (TNFα, Mm00443258_m1), and interleukin-1beta (IL-1β, Mm01336189_m1) were purchased from Applied Biosystems Inc. In addition, primer and Hex-labeled probe sets for 28S rRNA (Forward: 5'-CGGCTACCACATCCAAGGAA-3', Reverse: 5"-GCTGGAATTACCGCGGCT-3', Probe: 5HEX-TGCTGGCACCAGACTTGCCCTC-IABkFQ) were purchased from Integrated DNA Technologies (IDT, Coralville, IA). All RT-qPCR reactions contained TaqMan® 2X Universal PCR Mastermix, 5 μl diluted cDNA, 1 μl each of the TaqMan® primer and IDT primer and probe sets, and RNAse free water for a total volume of 20 μl. For these RT-qPCR reactions, an Applied Biosystems Model 7900HT kinetic PCR instrument was employed. The TaqMan® PCR reaction conditions were as follows: 2 min at 50°C (AmpErase UNG incubation), 10 min at 95°C (activation of AmpliTaq Gold and inactivation of AmpErase UNG), followed by 40 cycles each 15 s at 95°C and 1 min at 60°C on Micro Amp Optical 96-well plates.

Relative levels of P2Y12, Itgβ2, TNFα, and IL-1β mRNA were determined by normalizing against the expression of the 28S rRNA control present in each reaction. ΔΔCt values were calculated by subtracting the Ct value for internal control (rRNA) from the Ct value of the target gene. Relative gene expression for each gene was calculated using the average Ct value of control group with the $2^{-\Delta\Delta Ct}$ formula (Applied Biosystems). Data from 5-8 animals were pooled and analyzed for each condition, genotype, and time point. All results are reported as the mean ± standard error of the mean (SEM). Statistical significance was assessed using two-tailed t-tests. For data presented in Fig. 4, a Bonferroni correction for multiple hypotheses was conducted using a family size of four, based on the comparison between PBS- and EtOH-injected animals at each of four time-points. P values ≤ 0.05 were considered statistically significant.

Results

Timing of Apoptotic Cell Death and Clearance Following Acute Ethanol Exposure in Neonatal Mice

In the developing mouse, the so-called "brain growth spurt" occurs during the first and second postnatal weeks (Dobbing and Sands, 1979), which corresponds developmentally to the third fetal trimester in the human (Rice and Barone, 2000). During this time of rapid brain growth, neuronal connections are made and remodeled, and some post-mitotic neurons are eliminated via caspase-mediated apoptosis (Oppenheim, 1991). Previous work in rat (Ikonomidou et al., 2000) and mouse (Olney et al., 2002) models suggested that acute EtOH exposure at this developmental stage (P7) induces widespread neuronal apoptosis in the neocortex by activating caspase-3, an executioner caspase (Carloni et al., 2004; Han et al.,

2005). The level of this alcohol-induced neuroapoptosis has also been shown to scale with the level of blood alcohol (Ikonomidou et al., 2000). To confirm and extend these results, we used antibodies against the active, cleaved form of caspase-3 (CC3) to assess the timing and prevalence of apoptotic cell death initiated in the developing somatosensory cortex following acute EtOH exposure at two different EtOH concentrations, 3 g/kg (Fig. 1) and 5 g/kg (Fig. 2).

Cleaved Caspase 3

In control mouse pups injected with PBS on P7 and sacrificed 6-12 h later, there were very few CC3+ cells in the neocortex (Figs. 1A and 2A), and these few cells were typically located in cortical layers II and IV (Figs. 1C, PBS and 2C, PBS). These CC3+ cells likely reflect naturally apoptotic cells because un-injected pups showed similar patterns and levels of CC3 staining (data not shown), corresponding to cortical layers of highest natural cell death at this developmental stage (Ferrer et al., 1990, 1992). In contrast, injection of 3 or 5g/kg EtOH substantially increased the number of CC3+ cells (Figs. 1B and 2B), which again were primarily located in cortical layers II and IV (Figs. 1C, EtOH 6 h and 2C, EtOH 12 h). Higher magnification images of cortex taken 4 to 12 h after EtOH injection indicate that many CC3+ cells in cortical layer IV had a pyramidal shaped soma, often with beaded apical dendrites, suggestive of early stages of degeneration. The number of pyramidal-like CC3+ cells in layer IV decreased by 24 h after 3 or 5 g/kg EtOH-injection, although a collection of small CC3+ cell fragments remained. These small CC3+ structures were likely remnants of apoptotic bodies derived from dying cells. There was a further reduction in the number of CC3+ particles at 48 h (Figs. 1C, Top Row and 2C, Top Row). Quantitative particle analyses of CC3+ structures in cortical layer IV, just lateral to the cingulate gyrus (Figs. 1B,D and 2 B,D), indicated a significant increase in CC3+ structures at 6 and 12 h (22.3 ± 6 and 12.5 ± 6.3 particles/focal plane, respectively) following injection with 3g/kg EtOH, with a decrease to near baseline levels at 24 h (Fig. 1E). Likewise, following 5 g/kg EtOH injection there was a significant increase in CC3+ structures at 12 h (110.8 ± 38.8 particles/focal plane). There was a trend toward a significant increase in CC3+ structures at 24 (13.7 ± 10.9) and 48 h (2.80 ± 1.7) post-EtOH injection relative to time-matched PBS-injected controls, although these values did not reach statistical significance (Fig. 2E). Western blot analysis of CC3 levels in whole cortex corroborates the results of the particle analyses for CC3 (Figs. 1F and 2F). These results are consistent with the idea that the level of neuroapoptosis following developmental EtOH exposure scales with BACs (Ikonomidou et al., 2000) as there was a significant ($p = 0.0005$), nearly 10-fold, increase in density of CC3+ structures at 12 h in the cortex of mice exposed to 5 g/kg EtOH relative to those exposed to 3 g/kg EtOH.

PSVue

CC3 is an early and transient marker of the apoptotic cascade but may also label cells that, while stressed, recover and avoid an irreversible path to cell death (Snigdha et al., 2012). Externalization of phosphatidylserine (PS) occurs later than caspase activation and may be dependent on it; therefore, PS externalization is a more reliable indicator of cell commitment to an apoptotic pathway (Elmore, 2007). Consequently, we used PSVue, a fluorescent probe that binds with high affinity to PS, to identify and track cells in the later stages of apoptosis.

As was seen by CC3 staining, at 6 to 12 h after PBS-injection, PSVue+ structures were loosely scattered but somewhat concentrated within cortical layers II and IV (Figs. 1C and 2C, Middle Rows). PSVue+ structures were typically smaller than CC3+ structures, consistent with being late stage apoptotic bodies. Similar to that observed with CC3 staining, the density of PSVue+ structures appeared to increase compared to PBS-injected controls at 6 and 12 h after 3 and 5 g/kg EtOH injection, respectively. However, unlike CC3, the density of PSVue-labeled structures continued to increase at 24 h following 5 g/kg EtOH. By 48 after 3 g/kg and 96 h after 5 g/kg EtOH exposure, there were few PSVue labeled structures remaining in the cortex, consistent with their having been phagocytically removed. A quantitative particle analysis in cortical layer IV indicated a significant increase in PSVue+ structures relative to the time-matched PBS-injected control at 6 h (11.8 ± 5.3 particles/focal plane) and 12 h (22.7 ± 11.3) after 3g/kg EtOH (Fig. 1G), and at 12 h (31.8 ± 13.6) and 24 h (221.7 ± 157.4) after 5 g/kg EtOH (Fig. 2G). As with CC3, the density of PSVue+ structures returned to baseline by 48 and 96 h after 3 and 5 g/kg EtOH, respectively. These results further support the idea that neurodegeneration scales with BACs (Ikonomidou et al., 2000) as there was a significant ($p = 0.03$), over 10-fold, increase in density of PSVue+ structures at 24 h in the cortex of animals exposed to 5 g/kg EtOH relative to those exposed to 3 g/kg EtOH. Moreover, they demonstrate nearly complete clearance of apoptotic cells within ~2 d after acute alcohol exposure.

Microglial Activation, Interaction with Apoptotic Cells, and Deactivation Following Acute Ethanol Exposure

The results above demonstrate that acute exposure to moderate or high levels of EtOH induces a transient increase in apoptotic cell death. As the principal phagocytes in the brain (Sierra et al., 2013), microglia are likely responsible for the removal of dead cells from the cortex after EtOH exposure. However, while the phagocytic activity of microglia during chronic EtOH exposure has been studied in cell culture (Aroor and Baker, 1998; Colton et al., 1998), little is known regarding how acute EtOH exposure affects microglia structure and function *in situ*. Therefore, we assessed morphological and molecular aspects of microglial activation and examined the physical interactions of microglia with dead and dying cells following EtOH exposure *in situ*.

Morphological evidence for microglial activation and deactivation

To visualize microglia morphology and distribution, we used heterozygous GFP-reporter mice ($CX3CR1^{GFP/+}$) in which GFP is expressed in parenchymal microglia. Although GFP is also expressed in some perivascular cells that line larger brain blood vessels, as well as in cells in the meningeal layers at the cortical surface, the flattened morphology and location of these cells make them easy to distinguish from ramified parenchymal microglia.

In PBS-injected neonatal (P7) control mice, GFP-expressing microglia had a primitive ramified morphology and were scattered with significant space between cells, typical of this stage of rodent development (Dalmau et al., 1998, 2003). As development proceeded over the next several postnatal days, the density of microglia increased somewhat and microglial cell bodies decreased in size with a concomitant elaboration of fine branches. However,

microglia remained evenly distributed with non-overlapping branching arbors (Fig. 3A and B, PBS).

Following both 3 and 5 g/kg EtOH-injection on P7, cortical microglia underwent changes in cell structure that are typical of activation. In contrast to the primitive ramified morphology microglia maintained in the presence of the low levels of developmental cell death (Fig. 3A and B, PBS), some microglia retracted their branches and assumed a more amoeboid morphology by 12 and 24 h following 3 and 5 g/kg EtOH-injection, respectively (Fig. 3A and B, EtOH). This morphological transformation was particularly pronounced in cortical layer IV, and to a lesser extent layer II, corresponding to regions of highest EtOH-induced apoptosis (cf. Figs. 1 and 2). In addition, the density of amoeboid microglia appeared to increase, especially in cortical layer IV, and decrease in adjacent layers. This was especially apparent following 5 g/kg EtOH exposure. However, these changes in microglial morphology and distribution were transient and began to reverse after 24 and 48 h following either 3 and 5 g/kg EtOH exposures, respectively, coincident with a reduction in the density of dead cell debris (cf. Figs. 1C and 2C). Thus, by 2 and 4 days after 3 and 5 g/kg EtOH exposure, respectively, microglia were redistributed in the cortical layers and were once again highly ramified, and essentially indistinguishable from age-matched controls (Fig. 3A and B, PBS vs EtOH). Finally, analysis of microglial cell density in cortical layer IV showed no significant difference when assessed 96 h after PBS or EtOH (5 g/kg) injection (Suppl. Fig. 1). These data show reversible morphological changes in microglia following both 3 and 5 g/kg EtOH-exposure.

Molecular evidence for microglial activation and deactivation

The levels of several microglial-specific proteins change with classical microglial activation. Microglial expression of the CR3/MAC-1 β2-integrin subunit (Itgβ2) typically increases with activation (Kurpius et al., 2006), whereas expression of the purinergic receptor, P2Y12, decreases with activation (Haynes et al., 2006). Therefore, we examined the extent to which EtOH causes changes in expression of these microglial-specific genes. RT-qPCR analyses of mRNA levels in whole cortical tissues derived from PBS- and EtOH-injected animals demonstrate a significant decrease in P2Y12 expression at 12 h (0.4 ± 0.08 fold relative to PBS control) after 3 g/kg EtOH injection (Fig. 4A). Similarly, P2Y12 expression was also decreased at 12 h (0.6 ± 0.03) and 24 h (0.4 ± 0.04) after 5 g/kg EtOH injection (Fig. 4B). Typical of classical microglial activation, the decrease in P2Y12 expression was accompanied by a concomitant increase in Itgβ2 mRNA levels at 24 h (2.6 ± 0.4) and 48 h (2.7 ± 0.4) following 5 g/kg EtOH exposure (Fig. 4B). However, following 3 g/kg EtOH exposure Itgβ2 did not increase, but instead was significantly reduced (0.6 ± 0.04) at 6 h after EtOH injection (Fig. 4A). Despite these differences, by 24 h following 3 g/kg EtOH and 96 h following 5 g/kg EtOH, both P2Y12 and Itgβ2 expression were similar to that seen in PBS-injected controls, consistent with microglial deactivation (Fig. 4A,B). These changes in microglial gene expression were also visualized at the protein level using IHC in GFP-expressing mice (Fig. 4C). At 24 h following 5 g/kg EtOH exposure, P2Y12 immunoreactivity (IR) in GFP+ microglia decreased relative to age-matched PBS-injected controls (Fig. 4C, Left), while Itgβ2 expression increased relative to controls (Fig. 4C, Right). Levels of P2Y12 IR remained somewhat lower in EtOH-injected mice at 48 h, but

appeared to be returning to control levels as microglia re-ramify. In contrast, Itgβ2 expression remained elevated at 48 h after EtOH-injection. Examination of P2Y12 and Itgβ2 staining at higher magnification in GFP-expressing mice demonstrated that both stains co-localized specifically with microglial cells (Fig. 4C).

Pro-inflammatory factors

Activated microglia have been shown to release pro-inflammatory factors (PIFs) during pathology, and several studies have demonstrated an inflammatory response associated with developmental EtOH exposure using both *in situ* and cell culture models (Alfonso-Loeches et al., 2010; Boyadjieva and Sarkar, 2010, 2013; Fernandez-Lizarbe et al., 2009, 2013; Tiwari and Chopra, 2011). Therefore, we examined the extent to which different levels of acute EtOH exposure *in situ* change the expression of two prominent inflammatory factors, TNFα and IL-1β, which are produced by microglia (Colton and Wilcock, 2010). RT-qPCR analysis of gene expression in whole cortical tissues (same cDNA as those used to examine microglial activation markers) showed that neither TNFα nor IL-1β expression changed significantly following injection of 3 g/kg EtOH (Fig. 4D). In contrast, following injection of 5 g/kg EtOH, TNFα was significantly increased at both 12 (7.8 ± 0.6 fold increase) and 24 h (11.7 ± 2.4) (Fig. 4E). IL-1β expression was also significantly increased at 24 h (16.9 ± 5.4). mRNA levels of both TNFα and IL-1β were similar to baseline at 48-96 h following 5 g/kg EtOH. We confirmed that the pro-inflammatory factors measured in these analyses are derived from the cortical parenchymal tissues and not from any residual blood as animals perfused with PBS prior to sacrifice showed similar levels of TNFα as those that were unperfused (Suppl. Fig. 2).

Together, these results provide correlative morphological and molecular evidence indicating a concentration-dependent response of microglia to EtOH exposure in neonatal mice. These data suggest a rapid but reversible classical microglial activation and PIF expression following 5 g/kg acute EtOH-exposure in the developing cortex. Like microglia exposed to 5 g/kg EtOH, following 3 g/kg EtOH microglia appear to undergo a rapid but reversible activation cycle. However, cortical microglial activation following 3 g/kg EtOH is dampened and shows an altered, non-classical expression pattern for Itgβ2, TNFα, and IL-1β, when compared to their 5 g/kg counterparts.

Microglial activation and deactivation correlates with clearance of apoptotic cells

As brain phagocytes, activated microglia typically up-regulate a highly-glycosylated lysosomal protein (Kurpius et al., 2006), known as macrosialin, a homolog of human CD68 (Damoiseaux et al., 1994) that recognizes PS-rich structures (Ramprasad et al., 1995). By IHC, we observed low but detectible levels of CD68 IR in the cortical mantle of control brain tissues during the second post-natal week (Fig. 5A and B, PBS), presumably reflecting a basal level of phagocytic removal of naturally apoptotic cells. Much higher levels of CD68 immunostaining were found in the underlying corpus callosum (CC), where many activated microglia accumulate at this developmental stage (Ling, 1976). Following both 3 and 5 g/kg ethanol exposure, the intensity of CD68 immunostaining substantially increased in the cortical mantle, especially in cortical layers II and IV, up to 24 h after EtOH injection (Fig. 5A and B, EtOH). CD68 up-regulation was stronger and persisted longer following the 5

g/kg EtOH exposure. CD68 IR decreased to near control levels at 48 h for 3 g/kg, and at 96 h for 5 g/kg (Fig. 5A and B, PBS and EtOH). Examination of CD68 staining at higher magnification in cortical layer IV of GFP-expressing mice demonstrated that primitive ramified microglia in control tissues express a low level of punctate staining, and that after EtOH (5 g/kg) strong CD68 immunostaining colocalized to activated, amoeboid microglial cells (Fig. 5B, Cortical Layer IV). Further, analysis demonstrated a spatial relationship between CD68 and microglial phagocytosis (Fig. 5C). In particular, although CD68 was not strictly colocalized with PSVue structures in phagosomes, it was often seen surrounding microglial phagocytic profiles (Fig. 5C, Overlay and plot profile). These data suggest that, following acute EtOH exposure, activated microglia *in situ* transiently up-regulate proteins associated with degradation of dead cell debris, and this is spatially and temporally correlated with the presence of apoptotic cells.

Microglia engagement of apoptotic cells

To more directly examine the timing of microglial interactions with apoptotic cells, tissues from GFP-reporter mice were double-labeled with anti-CC3 and PSVue. Confocal images in cortical layer IV of PBS-injected mice showed some small PSVue+ particles and a few larger, CC3+ pyramidal-like cells (Fig. 6A). Many of the PSVue+ particles were completely engulfed by microglial processes, but microglia only rarely contacted CC3+ structures. This pattern of selective microglial contact with later stage apoptotic cells was maintained even after EtOH exposure resulting in a much higher density of PSVue+ and CC3+ structures (Fig. 6B), irrespective of the time after EtOH exposure. At early time-points (4 h) after EtOH exposure, the structure of CC3-labeled pyramidal cell dendrites varied from smoothly tapering (Fig. 6C) to blebby or beaded (Fig. 6D), suggesting that many of the CC3+ cells were in the early stages of degeneration. Although some large cellular structures were labeled with both CC3 and PSVue (Fig. 6E), this was rare, and most PSVue+ structures were small, condensed profiles characteristic of late stage degenerating cells or apoptotic bodies (Fig. 6A-B, F-G). Sometimes, small PSVue+ structures were aligned in linear arrays suggestive of fragmented dendrites (Suppl. Fig. 3). Not all PSVue+ structures were contained within microglia (Fig. 6A and B), indicating that PSVue labeling is not simply a result of degradation within microglia phagosomes. These *in situ* observations are in agreement with previous studies in cell culture showing that microglial phagocytosis of apoptotic cells begins after the cell is already committed to an apoptotic fate, corresponding in time with PS externalization (Adayev et al., 1998) and PSVue staining.

Microglial Activation and Pro-inflammatory Factor Expression are Driven Largely and Indirectly by Apoptotic Cell Death, not the Ethanol

Microglial activation and mobilization following acute EtOH-exposure *in vivo* could result from a direct action of the EtOH, an indirect action via cell death, or both. To determine the extent to which EtOH induces microglial activation *in situ* in the absence of apoptotic cell death (neuronal or non-neuronal), we generated heterozygous GFP-reporter mice deficient in BAX ($CX3CR1^{GFP/+}$:$BAX^{-/-}$) and injected these mice with PBS or EtOH. For these experiments we used the higher EtOH concentration (5 g/kg) in an effort to induce stronger microglial activation and PIF expression. Analysis of CC3 immunostaining in PBS-injected (Fig. 7A, PBS) or un-injected (not shown) mice showed that natural developmental

apoptosis is essentially abolished in BAX nulls. Only rarely was there a PSVue+ profile, indicating a very low level of spontaneous developmental cell death in these mice. Consistent with a previous study (Young et al., 2003), BAX knockout prevented the EtOH-induced neuronal apoptosis (Fig. 7A, EtOH).

Analyses of GFP-expressing mice showed that loss of BAX largely prevented changes in microglia morphology and accumulation in cortical layers II and IV typically seen at 24 h following 5 g/kg EtOH injection (Fig. 7B, EtOH). These morphological data were corroborated by RT-qPCR analyses of P2Y12 and Itgβ2 expression at 24 h, which showed that the typical changes in microglial gene expression induced by 5 g/kg EtOH were abrogated in the BAX KO mice (Fig. 7C). Likewise, immunohistochemical staining showed that the increase in microglial CD68 expression typically seen in the cortical mantle (especially layer IV) at 24 h following 5 g/kg EtOH injection (Fig. 7D, WT) was absent in BAX KO mice (Fig. 7D, KO). Finally, RT-qPCR analyses of TNFα and IL-1β expression at 24 h after EtOH injection demonstrated that the increase in inflammatory signals is largely abrogated in BAX KO mice (Fig. 7E). However, there is a minor, but statistically significant, residual increase in IL-1β (1.5 ± 0.1 fold increase), but no significant increase in TNFα.

Together, these data indicate that the rapid and robust microglial activation and PIF expression observed *in situ* following acute EtOH exposure is largely driven indirectly by BAX-dependent apoptotic cell death, rather than directly by the EtOH.

Discussion

Here we used a mouse model of FASD to study microglial responses to acute alcohol exposure during peak periods of cortical growth *in situ*. We show that alcohol-induced microglial activation in the developing neocortex is dose-dependent, rapid in onset, spatially correlated with degenerating neurons, and reversible. A comparison of *in situ* microglial responses to 3 and 5 g/kg alcohol is summarized in Fig. 8. Within the first few hours after EtOH exposure in both 3 and 5 g/kg paradigms, microglia retract their branches and down-regulate expression of P2Y12 while simultaneously up-regulating lysosomal proteins (CD68), changes that signify microglial activation. In addition, microglia accumulate in cortical layers II and IV, which show high levels of apoptotic cell death. Microglia contact and engulf apoptotic cells that externalize PS, after which they deactivate and quickly assume a normal tiled distribution within the cortex. However, microglial responses to the two concentrations of alcohol are not identical and show three major differences. First, while microglia become transiently activated in response to both alcohol concentrations, the period of microglial activation is shorter following 3 g/kg EtOH (24 h) when compared to 5 g/kg EtOH (48 h). Second, while microglia up-regulate cell adhesion molecules (β2 integrins) after 5 g/kg alcohol exposure, typical of classical activation, microglia down-regulate these proteins following exposure to 3 g/kg alcohol (Fig. 8, Microglial Activation Expression Profile). Third, while the timing of microglial activation and deactivation correlates with the transient expression of pro-inflammatory factors (TNFα and IL-1β) following 5 g/kg EtOH, the expression of these factors does not change significantly following exposure to 3 g/kg EtOH (Fig. 8, Inflammation Expression Profile). Experiments in BAX null mice strongly

suggest that microglial activation and expression of PIFs *in situ* is induced primarily by neurodegeneration. Together, these observations define spatially- and temporally-resolved responses of microglia to acute alcohol exposure in developing neocortex, discriminate between direct and indirect effects of alcohol on microglia, and uncover a remarkable reversibility of microglial activation in the cortex *in situ* following an acute neonatal alcohol exposure.

Timing of Alcohol-induced Microglial Activation and Clearance of Dead Cells

Previous studies used CC3 immunohistochemistry and silver staining to define spatial and temporal patterns of cell death in rodents following post-natal alcohol exposure (Coleman et al., 2012; Olney et al., 2002). However, the process of dead cell clearance after alcohol exposure has remained largely unexplored. This is important to define because alcohol may disrupt microglial phagocytosis, including the active movements by which microglia find and engage dead cells (Stence et al., 2001; Petersen and Dailey, 2004), and delayed clearance of apoptotic cells may cause further tissue damage (Chekeni and Ravichandran, 2011). Saito et. al. (2010) began to address the question of whether microglia phagocytose and clear dead cells when they demonstrated a colocalization between Iba-1 and phosphorylated tau staining in the cingulate cortex of mice during the first 24 h following 5 g/kg alcohol exposure. However, the timecourse of debris removal was not reported. Therefore, to determine the timing of cell death and subsequent dead cell clearance, we used two different markers of cell death: anti-CC3 immunostaining, which marks early stage apoptotic cells, and PSVue, a marker of later stages of apoptosis. Comparison of CC3 and PSVue labeling aided in the identification of spatial and temporal patterns of neuronal cell death and clearance. The low level of CC3 observed at 24 h after EtOH exposure suggests that EtOH toxicity has run its course and that subsequently there is little new cell death. Our data suggest that, in contrast to CC3, PSVue labels apoptotic cells throughout the later stages of cell death. Therefore, PSVue not only acts as a marker of dead cells, its loss can be used to monitor clearance of dead cells. The reduction in PSVue+ structures from 12 through 48 h following 3 g/kg EtOH and 24 through 96 h following 5 g/kg EtOH indicates that apoptotic cells are cleared from the cortex over these time periods and that final clearance is slower with higher levels of cell death. Thus, increasing levels of cell death lead to more extended periods of time over which dead cell debris may potentially promote secondary damage.

There is growing evidence that microglia are critical for normal CNS development, playing roles in synapse remodeling, angiogenesis, and developmental apoptosis (Eyo and Dailey, 2013). Microglia have long been implicated in the clearance of naturally apoptotic neurons during brain development (Ferrer et al., 1990), and cell culture studies have implicated PS as an “eat me” signal on apoptotic neurons recognized by microglia (Marin-Teva et al., 2004; Witting et al., 2000). Using GFP-reporter mice and multi-channel confocal imaging of CC3 and PSVue, we show here that microglia *in situ* contact and phagocytose apoptotic cells after they externalize PS. First, we showed that following 3 or 5 g/kg alcohol exposure, CD68 IR increased in microglia where it was often seen surrounding large phagocytic profiles. However, much CD68 IR was not strictly colocalized with PSVue in phagocytic structures. It may be that CD68 associates with phagocytosed material only at later stages of

digestion in the lysosome. Further analyses of microglial interactions with apoptotic cells under control conditions suggested that microglia preferentially contact PSVue+ cells, as the majority of PSVue+ cells were either surrounded by microglial processes or found within microglia branches or cell bodies. In contrast, microglia rarely contacted CC3+ cells, and CC3+ structures were almost never seen within microglia. This pattern of cell-cell interaction also occured following EtOH exposure, with the exception that while microglia maintained a bias for contacting PSVue+ cells, at peak periods of cell death there was a large fraction of PSVue+ profiles outside of microglia. This suggests that, following alcohol exposure, cell death exceeds the capacity of microglia to immediately clear them. These data indicate that microglia, whether during normal development or following alcohol exposure, are phagocytically engaged with later stage (PSVue+) apoptotic profiles. The high phagocytic activity of microglia suggests that they promote restoration of homeostasis in the developing neocortex following acute alcohol exposure. Although our observations do not rule out a role for microglia in the demise of vulnerable neurons (Marin-Teva et al., 2004; Neher et al., 2012), the morphology of the PSVue+ structures contacted by microglia suggests that microglia *in situ* initiate phagocytosis of apoptotic cells after they commit to an apoptotic fate. This is in agreement with cell culture studies showing that neonatal mouse brain microglia phagocytose only late stage apoptotic neurons after they externalize PS (Adayev et al., 1998).

Acute Developmental Alcohol Exposure in situ Kills Cortical Neurons but not Microglia

A previous study using *in vitro* cell culture and an *in situ* mouse model of repeated alcohol exposure (3.5 g/kg applied daily on P3-5) showed significant loss of both neurons and microglia in the cerebellum (Kane et al., 2011). We found little evidence of microglial cell death in the neocortex following one day of alcohol exposure on P7 or P8, even when high levels of alcohol (5 g/kg) were applied. We rarely observed blebbed microglia, or CC3+ staining within microglia, suggesting that cortical microglia do not undergo intrinsic (CC3-mediated) apoptosis in this model of acute alcohol exposure. In addition, although we often found PSVue staining within microglia, this was typically in the form of small PSVue+ structures enveloped by microglial processes, indicating phagocytosis of other cells and not microglial cell death. Finally, microglial cell counts in the cortex at 96 h after 5 g/kg alcohol or PBS exposure show no change in microglial cell density (Suppl. Fig. 1). Differences in our results and previous work may relate to the developmental stage (P3-P5 vs. P7 or P8), the brain region examined (cerebellum vs. neocortex), *in situ* versus *in vitro* setting, and/or the level or duration of alcohol exposure (3 days vs. 1 day). Nevertheless, our data indicate that developing cortical microglia *in situ* can survive brief periods of high alcohol that are sufficient to induce widespread neuronal apoptosis.

Acute Developmental Alcohol Exposure In situ Induces Transient Microglial Activation

A previous study in which rat pups were injected daily with alcohol (5 g/kg) on postnatal days 7-9 demonstrated that TNFα, IL-1β, and TGF-β were significantly up-regulated when assessed 19 days after alcohol injection (Tiwari and Chopra, 2011). Although earlier time-points were not examined, these findings may indicate a prolonged period of microglial activation following repeated alcohol exposure, since activated microglia are commonly associated with the release of these PIFs (Colton and Wilcock, 2010). Because an anti-

inflammatory agent, resveratrol, reduced the alcohol-induced PIF expression and partially reversed behavioral memory deficits, it was suggested that microglial activation may exacerbate neuronal injury (Tiwari and Chopra, 2011). In contrast, in our acute alcohol exposure model we observed re-ramification and re-distribution of microglia throughout the cortical layers within a few days after alcohol exposure, indicating rapid microglial deactivation. This was corroborated at the molecular level by our observation that microglia revert back to a resting state molecular profile with a return of P2Y12, TNFα, IL-1β, Itgβ2, and CD68 expression to near baseline levels within 48 h following 3 g/kg EtOH and 96 h following 5 g/kg EtOH exposure. To our knowledge, this is the first demonstration of rapid microglial deactivation following neuronal injury in developing brain *in situ*.

Several signaling molecules including TGF-β, IL-10, TREM2, and DAP12 have been suggested to restrain or reverse microglial activation (Saijo and Glass, 2011; Spittau et al., 2013). Although we found no significant increase in expression of either TGF-β or IL-10 by RT-qPCR, preliminary microarray analysis of cortical tissues isolated from mice at 24 h after 5 g/kg alcohol exposure indicates an approximate 2-fold increase in the expression of triggering receptor expressed by myeloid cells-2 (TREM2) and its adaptor protein, DAP12 (data not shown). These factors may be of particular interest because they are important for microglial phagocytosis of apoptotic cells (Neumann and Takahashi, 2007) and can suppress TLR signaling (Hamerman et al., 2006; Turnbull et al., 2006), which promotes microglial release of inflammatory cytokines following alcohol exposure (Fernandez-Lizarbe et al., 2013). Future work will be required to confirm the up-regulation of TREM2 and DAP12 and to investigate their roles in regulating microglial responses to alcohol-induced neurodegeneration.

Although we have described here a transient and reversible microglial activation and PIF expression following acute neonatal alcohol exposure, as noted above others have demonstrated elevated PIF expression 21 days after three sequential days of alcohol exposure in neonatal (P7-9) rat (Tiwari and Chopra, 2011). In adolescent (P35) rat, a 4 day binge-like ethanol exposure (peak BAC 304-410 mg/dl) triggered partial microglial activation in the hippocampus that persisted through early adulthood, but TNF levels were unaltered when assessed two days after ethanol exposure (McClain et al., 2011). In adult rat, TNF protein levels in brain were increased following ethanol exposure for 10 d but not after a single day exposure (Qin et al., 2008). However, another study in 8-week-old rats in which ethanol exposure (5 g/kg initially followed by 3 g/kg, producing a BAC of 37 mM) was done intermittently over several weeks showed only transient TNF and IL-1β expression (Zhao et al., 2013). It seems likely that differences in transient versus prolonged inflammation are related to the age of the animal as well as the duration and pattern of alcohol exposure. Consequently, the results of our study and of others need to be interpreted cautiously and do not necessarily represent the ethanol response of microglia or CNS inflammation in all other brain regions, in different stages of brain development, or under different alcohol exposure protocols in different species.

Alcohol-induced Microglial Activation is Driven Primarily by Neuroapoptotic Cell Death

Several previous studies showed that cultured microglia can be directly activated by alcohol in the absence of neurons or apoptotic neuronal cell death (Boyadjieva and Sarkar, 2010, 2013; Fernandez-Lizarbe et al., 2009, 2013). However, microglial responses to alcohol may differ *in situ*. Indeed, using BAX null mice, we found in neocortex that the molecular and morphological correlates of microglial activation were essentially abrogated in the absence of apoptosis, even when high doses (5 g/kg) of alcohol were introduced. This finding is consistent with Saito and colleagues who demonstrated that lithium treatment abrogates alcohol-induced neuronal cell death (Saito et al., 2007a,b; Sadrian et al., 2012) as well as microglial activation (Saito et al., 2010) in the neocortex of P7 mice. The differing results between *in vitro* cell culture and *in situ* studies may be due to different temporal profiles of alcohol exposure or to differences in cellular vulnerabilities of previously activated microglia (in cell culture) and naïve microglia in developing brain *in situ*. It is important to note that we cannot rule out some undetected, long-lasting effects of alcohol on microglia *in situ*. However, the present observations demonstrate a high tolerance of cortical microglia to acute alcohol exposure *in situ* and raise caution about extrapolating results from primary microglial cell culture to *in vivo* settings.

Acute Developmental Alcohol Exposure and Pro-inflammatory Factor Expression

It is well established that activated microglia can produce a plethora of chemokines and cytokines, including PIFs and their receptors (Otero and Merrill, 1994), and are thus both initiators and targets of autocrine and paracrine signals (Hanisch, 2002). Our RT-qPCR analyses show that microglial activation following high (5 g/kg) alcohol exposure coincides with expression of PIFs, including TNFα and IL-1β. This increase in PIF expression is largely abrogated in BAX null mice, suggesting that the pro-inflammatory response of alcohol is driven indirectly by neuroapoptosis, not directly by the alcohol. We favor a model in which alcohol induces BAX-dependent neuroapoptosis, which activates microglia. At high levels of alcohol-induced cell death, microglial responses include a transient increase in PIF expression. We acknowledge that this model challenges the current thinking that apoptotic cell death does not elicit a pro-inflammatory response by microglia. In fact, it has been previously shown that apoptotic cell death is usually associated with an anti-inflammatory response (Neumann et al., 2009). This appears to be what is happening following 3 g/kg acute alcohol exposure, because we see little change in the expression of TNFα and IL-1β. However, the BAX data clearly indicate that the up-regulation of TNFα and IL-1β following 5 g/kg alcohol exposure is, in fact, largely dependent on alcohol-induced apoptotic cell death. Potentially, the increased expression of pro-inflammatory factors following 5 g/kg alcohol exposure may result from the slower clearance of late-stage apoptotic cells. Due to the longer clearance period, some of these late stage apoptotic cells may become necrotic, thus inducing PIF expression.

The functional role of the pro-inflammatory response following injection of 5 g/kg alcohol remains unclear, but work from other groups indicates diverse actions by which PIFs may either exacerbate neuronal injury or facilitate restorative functions (Hanisch, 2002). For example, Boyadjieva and Sarkar (2010, 2013) demonstrated an increase in neuronal cell death when conditioned media from alcohol-exposed (230-460 mg/dL alcohol for 24 h)

primary microglia was applied to cultured hypothalamic neurons, and this increase in neuronal cell death was abrogated by immunoneutralization of TNFα. Moreover, Fernandez-Lizarbe et al. (2009, 2013) demonstrated that, in contrast to WT microglia, microglia deficient in TLR's 2 or 4 do not release PIFs and are not able to induce neuronal cell death following chronic alcohol exposure. These results suggest cytotoxic roles for PIFs. However, other lines of research indicate that PIFs, particularly TNFα, can promote both microglial clearance of dead cells (Smith et al., 1998; von Zahn et al., 1997) and neuronal survival (Bonthius et al., 2008, 2009; Cabal-Hierro and Lazo, 2012). In fact, we have previously shown that TNFα can promote the survival of neurons against alcohol toxicity *in vitro* (Bonthius et al., 2008, 2009). Here, our histological analyses in neocortex following 5 g/kg acute alcohol exposure showed very low levels of new cell death (CC3 immunostaining) during and after peak periods of PIF expression (>24 h), and in western blots we failed to detect an increase in caspase-8 activation (data not shown) indicative of inflammation-induced extrinsic modes of apoptosis (O'Connor, 2013). Thus, in this model of acute alcohol exposure, PIFs do not appear to induce secondary neurodegeneration in the neocortex. Differences in the reported effects of PIFs may relate to the levels, timing, or regional patterns of expression. Although the precise roles of PIFs will need to be established in future studies, our observations leave open the possibility that PIFs may play restorative functions in the cortex after acute alcohol exposure. This is in line with the suggestion that partially activated microglia may, in fact, promote recovery after alcohol exposure in young adult rat (Marshall et al., 2013).

Results of the present study have broader implications for understanding microglial responses to drug-induced neuronal apoptosis in the developing brain. Like alcohol, other drugs that are NMDA receptor antagonists and/or $GABA_A$ agonists, including general anesthetics and anti-epileptic drugs that have been utilized in pediatric and obstetric medicine (Creeley and Olney, 2013), can induce apoptotic cell death during the brain growth spurt in animal models (Bittigau et al., 2002; Ikonomidou et al., 1999; Istaphanous et al., 2011; Jevtovic-Todorovic et al., 2003; Rizzi et al., 2008, 2010; Young et al., 2005). Thus, a better understanding of the factors that regulate microglial responses to apoptotic neuronal cell death in developing brain may have direct clinical applications.

Supplementary Material

Refer to Web version on PubMed Central for supplementary material.

Acknowledgments

Funded by NIH grants R21 AA018823 to MED, R01 AA021465 to DJB , R21 AA018710 and R21 AA018711 to BK, and P30 DC010362 to the Iowa Center for Molecular Auditory Neuroscience (ICMAN, S. Green, PI). KA was supported by an Evelyn Hart Watson Summer Fellowship and a University of Iowa Graduate College Summer Fellowship. We thank Dr. Joshua Weiner for the gift of Bcl-2-associated X protein (BAX) deficient mice as well as Dr. Bernd Fritzsch for the gift of PSVue and advice on PSVue labeling. We thank Dr. Joshua Weiner, Austin Keeler, and Kar Men Mah for help with western blotting, Ms. Jo Mahoney for help with blood alcohol determination, Joshua Colvin for help with quantitation, and Samuel Lifton for help with statistical analyses.

Bibliography

Adayev T, Estephan R, Meserole S, Mazza B, Yurkow EJ, Banerjee P. Externalization of phosphatidylserine may not be an early signal of apoptosis in neuronal cells, but only the phosphatidylserine-displaying apoptotic cells are phagocytosed by microglia. J. Neurochem. 1998; 71:1854–1864. [PubMed: 9798909]

Aguzzi A, Barres BA, Bennett ML. Microglia: scapegoat, saboteur, or something else? Science. 2013; 339:156–161. [PubMed: 23307732]

Alfonso-Loeches S, Pascual-Lucas M, Blanco AM, Sanchez-Vera I, Guerri C. Pivotal role of TLR4 receptors in alcohol-induced neuroinflammation and brain damage. J. Neurosci. 2010; 30:8285–8295. [PubMed: 20554880]

Aroor AR, Baker RC. Ethanol inhibition of phagocytosis and superoxide anion production by microglia. Alcohol. 1998; 15:277–280. [PubMed: 9590511]

Bittigau P, Sifringer M, Genz K, Reith E, Pospischil D, Govindarajalu S, Dzietko M, Pesditschek S, Mai I, Dikranian K, Olney JW, Ikonomidou C. Antiepileptic drugs and apoptotic neurodegeneration in the developing brain. Proc. Natl. Acad. Sci. U. S. A. 2002; 99:15089–15094. [PubMed: 12417760]

Bonthius DJ, Bonthius NE, Li S, Karacay B. The protective effect of neuronal nitric oxide synthase (nNOS) against alcohol toxicity depends upon the NO-cGMP-PKG pathway and NF-kappaB. Neurotoxicology. 2008; 29:1080–1091. [PubMed: 18824032]

Bonthius DJ, Luong T, Bonthius NE, Hostager BS, Karacay B. Nitric oxide utilizes NF-kappaB to signal its neuroprotective effect against alcohol toxicity. Neuropharmacology. 2009; 56:716–731. [PubMed: 19135070]

Bonthius DJ, Tzouras G, Karacay B, Mahoney J, Hutton A, McKim R, Pantazis NJ. Deficiency of neuronal nitric oxide synthase (nNOS) worsens alcohol-induced microencephaly and neuronal loss in developing mice. Brain Res. Dev. Brain Res. 2002; 138:45–59. [PubMed: 12234657]

Boyadjieva NI, Sarkar DK. Microglia play a role in ethanol-induced oxidative stress and apoptosis in developing hypothalamic neurons. Alcohol. Clin. Exp. Res. 2013; 37:252–262. [PubMed: 22823548]

Boyadjieva NI, Sarkar DK. Role of microglia in ethanol's apoptotic action on hypothalamic neuronal cells in primary cultures. Alcohol. Clin. Exp. Res. 2010; 34:1835–1842. [PubMed: 20662807]

Cabal-Hierro L, Lazo PS. Signal transduction by tumor necrosis factor receptors. Cell. Signal. 2012; 24:1297–1305. [PubMed: 22374304]

Carloni S, Mazzoni E, Balduini W. Caspase-3 and calpain activities after acute and repeated ethanol administration during the rat brain growth spurt. J. Neurochem. 2004; 89:197–203. [PubMed: 15030404]

Chastain LG, Sarkar DK. Role of microglia in regulation of ethanol neurotoxic action. Int. Rev. Neurobiol. 2014; 118:81–103. [PubMed: 25175862]

Chekeni FB, Ravichandran KS. The role of nucleotides in apoptotic cell clearance: implications for disease pathogenesis. J. Mol. Med. (Berl). 2011; 89:13–22. [PubMed: 20809090]

Chen WJ, Maier SE, Parnell SE, West JR. Alcohol and the developing brain: neuroanatomical studies. Alcohol Res. Health. 2003; 27:174–180. [PubMed: 15303628]

Coleman LG Jr, Oguz I, Lee J, Styner M, Crews FT. Postnatal day 7 ethanol treatment causes persistent reductions in adult mouse brain volume and cortical neurons with sex specific effects on neurogenesis. Alcohol. 2012; 46:603–612. [PubMed: 22572057]

Colton CA, Snell-Callanan J, Chernyshev ON. Ethanol induced changes in superoxide anion and nitric oxide in cultured microglia. Alcohol. Clin. Exp. Res. 1998; 22:710–716. [PubMed: 9622454]

Colton CA, Wilcock DM. Assessing activation states in microglia. CNS Neurol. Disord. Drug Targets. 2010; 9:174–191. [PubMed: 20205642]

Creeley CE, Olney JW. Drug-Induced Apoptosis: Mechanism by which Alcohol and Many Other Drugs Can Disrupt Brain Development. Brain Sci. 2013; 3:1153–1181. [PubMed: 24587895]

Crews F, Nixon K, Kim D, Joseph J, Shukitt-Hale B, Qin L, Zou J. BHT blocks NF-kB activation and ethanol-induced brain damage. Alcohol. Clin. Exp. Res. 2006; 30:1938–1949. [PubMed: 17067360]

Dalmau I, Finsen B, Zimmer J, Gonzalez B, Castellano B. Development of microglia in the postnatal rat hippocampus. Hippocampus. 1998; 8:458–474. [PubMed: 9825958]

Dalmau I, Vela JM, Gonzalez B, Finsen B, Castellano B. Dynamics of microglia in the developing rat brain. J. Comp. Neurol. 2003; 458:144–157. [PubMed: 12596255]

Damoiseaux JG, Dopp EA, Calame W, Chao D, MacPherson GG, Dijkstra CD. Rat macrophage lysosomal membrane antigen recognized by monoclonal antibody ED1. Immunology. 1994; 83:140–147. [PubMed: 7821959]

Dobbing J, Sands J. Comparative aspects of the brain growth spurt. Early Hum. Dev. 1979; 3:79–83. [PubMed: 118862]

Drew PD, Kane CJ. Fetal alcohol spectrum disorders and neuroimmune changes. Int. Rev. Neurobiol. 2014; 118:41–80. [PubMed: 25175861]

Eggen BJ, Raj D, Hanisch UK, Boddeke HW. Microglial phenotype and adaptation. J. Neuroimmune Pharmacol. 2013; 8:807–823. [PubMed: 23881706]

Elmore S. Apoptosis: a review of programmed cell death. Toxicol. Pathol. 2007; 35:495–516. [PubMed: 17562483]

Eyo UB, Dailey ME. Microglia: key elements in neural development, plasticity, and pathology. J. Neuroimmune Pharmacol. 2013; 8:494–509. [PubMed: 23354784]

Fernandez-Lizarbe S, Montesinos J, Guerri C. Ethanol induces TLR4/TLR2 association, triggering an inflammatory response in microglial cells. J. Neurochem. 2013; 126:261–273. [PubMed: 23600947]

Fernandez-Lizarbe S, Pascual M, Guerri C. Critical role of TLR4 response in the activation of microglia induced by ethanol. J. Immunol. 2009; 183:4733–4744. [PubMed: 19752239]

Ferrer I, Bernet E, Soriano E, Del Rio T, Fonseca M. Naturally occurring cell death in the cerebral cortex of the rat and removal of dead cells by transitory phagocytes. Neuroscience. 1990; 39:451–458. [PubMed: 2087266]

Ferrer I, Soriano E, del Rio JA, Alcantara S, Auladell C. Cell death and removal in the cerebral cortex during development. Prog. Neurobiol. 1992; 39:1–43. [PubMed: 1589584]

Guizzetti M, Zhang X, Goeke C, Gavin DP. Glia and neurodevelopment: focus on fetal alcohol spectrum disorders. Front. Pediatr. 2014; 2:123. [PubMed: 25426477]

Hamerman JA, Jarjoura JR, Humphrey MB, Nakamura MC, Seaman WE, Lanier LL. Cutting edge: inhibition of TLR and FcR responses in macrophages by triggering receptor expressed on myeloid cells (TREM)-2 and DAP12. J. Immunol. 2006; 177:2051–2055. [PubMed: 16887962]

Han JY, Joo Y, Kim YS, Lee YK, Kim HJ, Cho GJ, Choi WS, Kang SS. Ethanol induces cell death by activating caspase-3 in the rat cerebral cortex. Mol. Cells. 2005; 20:189–195. [PubMed: 16267392]

Hanisch U-K. Microglia as a source and target of cytokines. Glia. 2002; 40:140–155. [PubMed: 12379902]

Harry GJ. Microglia during development and aging. Pharmacol. Ther. 2013; 139:313–326. [PubMed: 23644076]

Haynes SE, Hollopeter G, Yang G, Kurpius D, Dailey ME, Gan WB, Julius D. The P2Y12 receptor regulates microglial activation by extracellular nucleotides. Nat. Neurosci. 2006; 9:1512–1519. [PubMed: 17115040]

Ikonomidou C, Bosch F, Miksa M, Bittigau P, Vöckler J, Dikranian K, Tenkova T, Stevoska V, Turski L, Olney JW. Blockade of NMDA receptors and apoptotic neurodegeneration in the developing brain. Science. 1999; 283:70–74. [PubMed: 9872743]

Ikonomidou C, Bittigau P, Ishimaru MJ, Wozniak DF, Koch C, Genz K, Price MT, Stefovska V, Horster F, Tenkova T, Dikranian K, Olney JW. Ethanol-induced apoptotic neurodegeneration and fetal alcohol syndrome. Science. 2000; 287:1056–1060. [PubMed: 10669420]

Istaphanous GK, Howard J, Nan X, Hughes EA, McCann JC, McAuliffe JJ, Danzer SC, Loepke AW. Comparison of the neuroapoptotic properties of equipotent anesthetic concentrations of desflurane, isoflurane, or sevoflurane in neonatal mice. Anesthesiology. 2011; 114:578–587. [PubMed: 21293251]

Jevtovic-Todorovic V, Hartman RE, Izumi Y, Benshoff ND, Dikranian K, Zorumski CF, Olney JW, Wozniak DF. Early exposure to common anesthetic agents causes widespread neurodegeneration

in the developing rat brain and persistent learning deficits. J. Neurosci. 2003; 23:876–882. [PubMed: 12574416]

Jung S, Aliberti J, Graemmel P, Sunshine MJ, Kreutzberg GW, Sher A, Littman DR. Analysis of fractalkine receptor CX(3)CR1 function by targeted deletion and green fluorescent protein reporter gene insertion. Mol. Cell. Biol. 2000; 20:4106–4114. [PubMed: 10805752]

Kane CJ, Phelan KD, Drew PD. Neuroimmune mechanisms in fetal alcohol spectrum disorder. Dev. Neurobiol. 2012; 72:1302–1316. [PubMed: 22623427]

Kane CJ, Phelan KD, Han L, Smith RR, Xie J, Douglas JC, Drew PD. Protection of neurons and microglia against ethanol in a mouse model of fetal alcohol spectrum disorders by peroxisome proliferator-activated receptor-gamma agonists. Brain Behav. Immun. 2011; 25(Suppl 1):S137–45. [PubMed: 21376806]

Knudson CM, Tung KS, Tourtellotte WG, Brown GA, Korsmeyer SJ. Bax-deficient mice with lymphoid hyperplasia and male germ cell death. Science. 1995; 270:96–99. [PubMed: 7569956]

Kurpius D, Wilson N, Fuller L, Hoffman A, Dailey ME. Early activation, motility, and homing of neonatal microglia to injured neurons does not require protein synthesis. Glia. 2006; 54:58–70. [PubMed: 16715500]

Ling EA. Some aspects of amoeboid microglia in the corpus callosum and neighbouring regions of neonatal rats. J. Anat. 1976; 121:29–45. [PubMed: 1254530]

Marin-Teva JL, Dusart I, Colin C, Gervais A, van Rooijen N, Mallat M. Microglia promote the death of developing Purkinje cells. Neuron. 2004; 41:535–547. [PubMed: 14980203]

Marino MD, Aksenov MY, Kelly SJ. Vitamin E protects against alcohol-induced cell loss and oxidative stress in the neonatal rat hippocampus. Int. J. Dev. Neurosci. 2004; 22:363–377. [PubMed: 15380836]

Marshall SA, McClain JA, Kelso ML, Hopkins DM, Pauly JR, Nixon K. Microglial activation is not equivalent to neuroinflammation in alcohol-induced neurodegeneration: The importance of microglia phenotype. Neurobiol Dis. 2013; 54:239–51. [PubMed: 23313316]

May PA, Gossage JP, Kalberg WO, Robinson LK, Buckley D, Manning M, Hoyme HE. Prevalence and epidemiologic characteristics of FASD from various research methods with an emphasis on recent in-school studies. Dev. Disabil. Res. Rev. 2009; 15:176–192. [PubMed: 19731384]

McClain JA, Morris SA, Deeny MA, Marshall SA, Hayes DM, Kiser ZM, Nixon K. Adolescent binge alcohol exposure induces long-lasting partial activation of microglia. Brain Behav Immun. 2011; 25(Suppl 1):S120–8. [PubMed: 21262339]

Napoli I, Neumann H. Microglial clearance function in health and disease. Neuroscience. 2009; 158:1030–1038. [PubMed: 18644426]

Neumann H, Kotter MR, Franklin RJ. Debris clearance by microglia: an essential link between degeneration and regeneration. Brain. 2009; 132:288–295. [PubMed: 18567623]

Neumann H, Takahashi K. Essential role of the microglial triggering receptor expressed on myeloid cells-2 (TREM2) for central nervous tissue immune homeostasis. J. Neuroimmunol. 2007; 184:92–99. [PubMed: 17239445]

O'Connor JJ. Targeting tumour necrosis factor-alpha in hypoxia and synaptic signalling. Ir. J. Med. Sci. 2013; 182:157–162. [PubMed: 23361632]

Olney JW, Tenkova T, Dikranian K, Qin YQ, Labruyere J, Ikonomidou C. Ethanol-induced apoptotic neurodegeneration in the developing C57BL/6 mouse brain. Brain Res. Dev. Brain Res. 2002; 133:115–126. [PubMed: 11882342]

Oppenheim RW. Cell death during development of the nervous system. Annu. Rev. Neurosci. 1991; 14:453–501. [PubMed: 2031577]

Otero GC, Merrill JE. Cytokine receptors on glial cells. Glia. 1994; 11:117–128. [PubMed: 7927642]

Petersen MA, Dailey ME. Diverse microglial motility behaviors during clearance of dead cells in hippocampal slices. Glia. 2004; 46(2):195–206. [PubMed: 15042586]

Qin L, He J, Hanes RN, Pluzarev O, Hong JS, Crews FT. Increased systemic and brain cytokine production and neuroinflammation by endotoxin following ethanol treatment. J Neuroinflammation. 2008; 5:10. 18. [PubMed: 18348728]

Ramprasad MP, Fischer W, Witztum JL, Sambrano GR, Quehenberger O, Steinberg D. The 94- to 97-kDa mouse macrophage membrane protein that recognizes oxidized low density lipoprotein and

phosphatidylserine-rich liposomes is identical to macrosialin, the mouse homologue of human CD68. Proc. Natl. Acad. Sci. U. S. A. 1995; 92:9580–9584. [PubMed: 7568176]

Rice D, Barone S Jr. Critical periods of vulnerability for the developing nervous system: evidence from humans and animal models. Environ. Health Perspect. 2000; 108(Suppl 3):511–533. [PubMed: 10852851]

Rizzi S, Carter LB, Ori C, Jevtovic-Todorovic V. Clinical anesthesia causes permanent damage to the fetal guinea pig brain. Brain Pathol. 2008; 18:198–210. [PubMed: 18241241]

Rizzi S, Ori C, Jevtovic-Todorovic V. Timing versus duration: determinants of anesthesia-induced developmental apoptosis in the young mammalian brain. Ann. N. Y. Acad. Sci. 2010; 1199:43–51. [PubMed: 20633108]

Sadrian B, Subbanna S, Wilson DA, Basavarajappa BS, Saito M. Lithium prevents long-term neural and behavioral pathology induced by early alcohol exposure. Neuroscience. 2012; 206:122–135. [PubMed: 22266347]

Saijo K, Glass CK. Microglial cell origin and phenotypes in health and disease. Nat. Rev. Immunol. 2011; 11:775–787. [PubMed: 22025055]

Saito M, Mao RF, Wang R, Vadasz C, Saito M. Effects of gangliosides on ethanol-induced neurodegeneration in the developing mouse brain. Alcohol Clin Exp Res. 2007a; 31(4):665–74. [PubMed: 17374046]

Saito M, Chakraborty G, Mao RF, Wang R, Cooper TB, Vadasz C, Saito M. Ethanol alters lipid profiles and phosphorylation status of AMP-activated protein kinase in the neonatal mouse brain. J Neurochem. 2007b; 103(3):1208–18. [PubMed: 17683484]

Saito M, Chakraborty G, Mao RF, Paik SM, Vadasz C, Saito M. Tau phosphorylation and cleavage in ethanol-induced neurodegeneration in the developing mouse brain. Neurochem. Res. 2010; 35:651–659. [PubMed: 20049527]

Sierra A, Abiega O, Shahraz A, Neumann H. Janus-faced microglia: beneficial and detrimental consequences of microglial phagocytosis. Front. Cell. Neurosci. 2013; 7:6. [PubMed: 23386811]

Smith ME, van der Maesen K, Somera FP. Macrophage and microglial responses to cytokines in vitro: phagocytic activity, proteolytic enzyme release, and free radical production. J. Neurosci. Res. 1998; 54:68–78. [PubMed: 9778151]

Snigdha S, Smith ED, Prieto GA, Cotman CW. Caspase-3 activation as a bifurcation point between plasticity and cell death. Neurosci. Bull. 2012; 28:14–24. [PubMed: 22233886]

Spittau B, Wullkopf L, Zhou X, Rilka J, Pfeifer D, Krieglstein K. Endogenous transforming growth factor-beta promotes quiescence of primary microglia in vitro. Glia. 2013; 61:287–300. [PubMed: 23065670]

Stence N, Waite M, Dailey ME. Dynamics of microglial activation: A confocal time-lapse analysis in hippocampal slices. Glia. 2001; 33:256–266. [PubMed: 11241743]

Subbanna S, Shivakumar M, Umapathy NS, Saito M, Mohan PS, Kumar A, Nixon RA, Verin AD, Psychoyos D, Basavarajappa BS. G9a-mediated histone methylation regulates ethanol-induced neurodegeneration in the neonatal mouse brain. Neurobiol. Dis. 2013; 54:475–485. [PubMed: 23396011]

Tiwari V, Chopra K. Resveratrol prevents alcohol-induced cognitive deficits and brain damage by blocking inflammatory signaling and cell death cascade in neonatal rat brain. J. Neurochem. 2011; 117:678–690. [PubMed: 21375533]

Turnbull IR, Gilfillan S, Cella M, Aoshi T, Miller M, Piccio L, Hernandez M, Colonna M. Cutting edge: TREM-2 attenuates macrophage activation. J. Immunol. 2006; 177:3520–3524. [PubMed: 16951310]

von Zahn J, Möller T, Kettenmann H, Nolte C. Microglial phagocytosis is modulated by pro- and anti-inflammatory cytokines. Neuroreport. 1997; 8:3851–3856. [PubMed: 9462454]

Wilson DA, Peterson J, Basavaraj BS, Saito M. Local and regional network function in behaviorally relevant cortical circuits of adult mice following postnatal alcohol exposure. Alcohol. Clin. Exp. Res. 2011; 35:1974–1984. [PubMed: 21649667]

Witting A, Muller P, Herrmann A, Kettenmann H, Nolte C. Phagocytic clearance of apoptotic neurons by Microglia/Brain macrophages in vitro: involvement of lectin-, integrin-, and

phosphatidylserine-mediated recognition. J. Neurochem. 2000; 75:1060–1070. [PubMed: 10936187]

Wozniak DF, Hartman RE, Boyle MP, Vogt SK, Brooks AR, Tenkova T, Young C, Olney JW, Muglia LJ. Apoptotic neurodegeneration induced by ethanol in neonatal mice is associated with profound learning/memory deficits in juveniles followed by progressive functional recovery in adults. Neurobiol. Dis. 2004; 17:403–414. [PubMed: 15571976]

Young C, Klocke BJ, Tenkova T, Choi J, Labruyere J, Qin YQ, Holtzman DM, Roth KA, Olney JW. Ethanol-induced neuronal apoptosis in vivo requires BAX in the developing mouse brain. Cell Death Differ. 2003; 10:1148–1155. [PubMed: 14502238]

Young C, Roth KA, Klocke BJ, West T, Holtzman DM, Labruyere J, Qin YQ, Dikranian K, Olney JW. Role of caspase-3 in ethanol-induced developmental neurodegeneration. Neurobiol. Dis. 2005; 20:608–614. [PubMed: 15927478]

Zhao YN, Wang F, Fan YX, Ping GF, Yang JY, Wu CF. Activated microglia are implicated in cognitive deficits, neuronal death, and successful recovery following intermittent ethanol exposure. Behav Brain Res. Jan 1; 2013 2013 236(1):270–82. [PubMed: 22985845]

Main Points

- Acute alcohol exposure dose-dependently drives unique patterns of microglial activation and inflammation in developing mouse neocortex.
- Microglia activation is largely driven by BAX-mediated apoptosis and is reversed after clearance of dead cells.

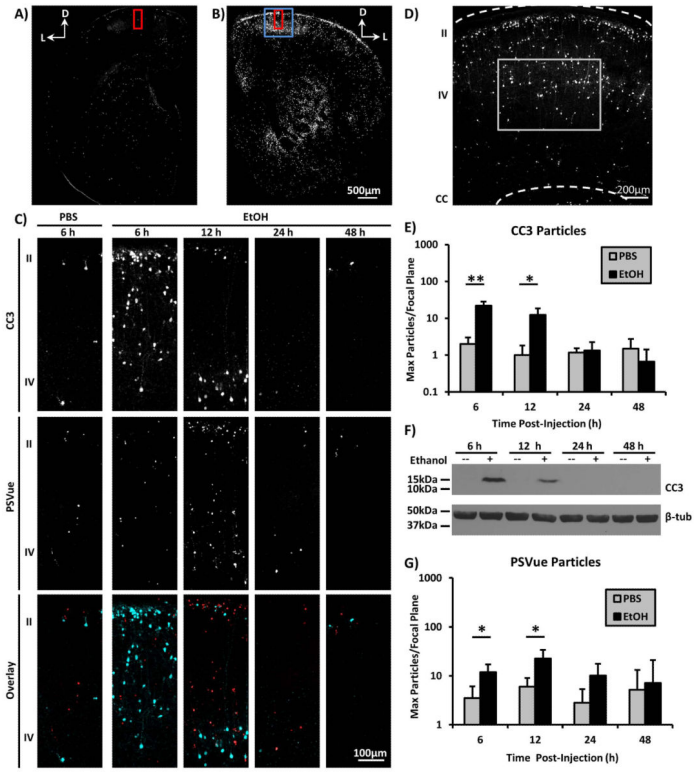

Figure 1. Acute 3 g/kg ethanol exposure in neonatal mice induces cortical apoptotic cell death

P7 mice were injected with PBS (**A**) or EtOH (**B**) and sacrificed 6 h later. Low magnification images show the distribution of anti-CC3 labeled cells in hemisections of the cerebrum at the level of the somatosensory cortex. At this magnification, few CC3+ cells are evident in PBS-injected controls (A), although many CC3+ cells are observed in cortical layers II and IV following EtOH-exposure (B). Images are Z-projections of confocal image stacks spanning 150 µm. D = dorsal; L = lateral. Red boxes in A and B indicate regions of the cortex shown in C. The blue box in B indicates the region of the cortex shown in D. (**C**) Higher magnification images showing apoptotic cells in layers II-IV of the cortex in animals injected with PBS and sacrificed 6 h later or injected with 3 g/kg EtOH and sacrificed 6, 12, 24, or 48 h later. Cells in early stages of apoptosis are labeled by anti-CC3 antibody (Top Row). Cells in later stages of apoptosis are labeled with PS-binding dye, PSVue (Middle Row). Overlay of CC3 (cyan) and PSVue (red) (Bottom Row). In PBS-injected controls, there is a low level of apoptotic cell death, which is concentrated in cortical layers II and IV. In EtOH-injected mice, there is an increase in both early (CC3+) and later-stage (PSVue+) apoptotic cells by 6 h (C, EtOH). Images are Z projections of confocal image stacks spanning 54 µm. (**D**) Boxed region shows the area in which CC3 and PSVue particle analyses were performed (E and G). (**E**) Particle analysis of CC3+ structures in cortical layer IV. Error bars represent SDP (N=4-6 cortical slices). * = 0.009, **p = 0.00009,. **F**) Western blot of CC3 protein in whole cortex following PBS (--) or EtOH (+) injection. β-tubulin was the internal loading control. Timeline of caspase-3 activation in whole cortex is in agreement with the immunohistochemical results shown in C. (**G**) Particle analysis of PSVue+ structures in cortical layer IV. Same tissue areas used for analysis as in (E). * < 0.05.

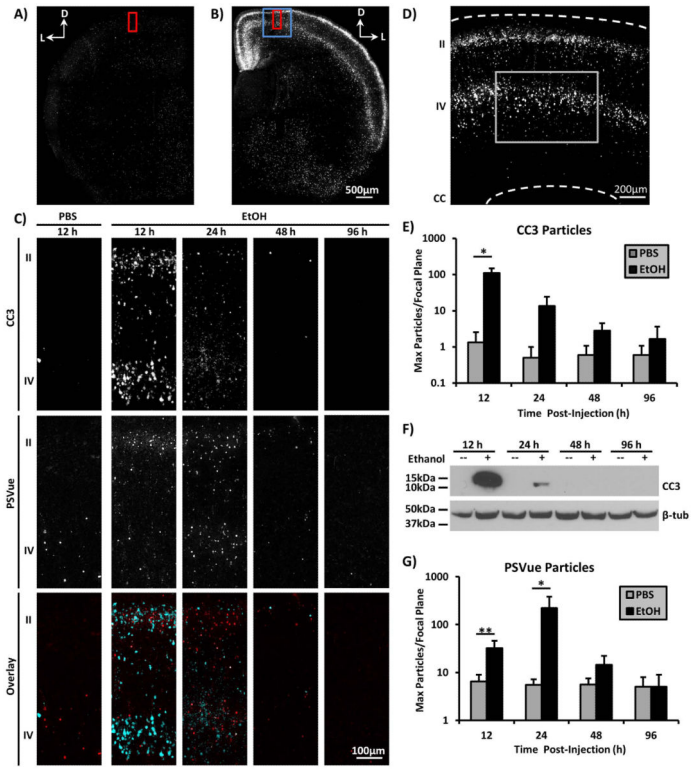

Figure 2. Acute 5 g/kg ethanol exposure in neonatal mice induces higher levels of cortical apoptotic cell death over a longer period of time

P7 mice were injected with PBS (**A**) or EtOH (**B**) and sacrificed 12 h later (A-B). Low magnification images show the distribution of anti-CC3 labeled cells in hemisections of thecerebrum at the level of the somatosensory cortex. At this magnification, few CC3+ cells are evident in PBS-injected controls (A), whereas many CC3+ cells are observed in cortical layers II and IV following EtOH-exposure (B). Images are Z projections of confocal image stacks spanning 150 μm. D = dorsal; L = lateral. Red boxes in A and B indicate regions of the cortex shown in C. The Blue box in B indicates the region of the cortex shown in D. (**C**) Higher magnification images showing apoptotic cells in layers II-IV of the cortex in animals injected with PBS and sacrificed 12 h later or injected with 5 g/kg EtOH and sacrificed 12, 24, 48, or 96 h (4 d) later. Cells in early stages of apoptosis are labeled by anti-cleaved caspase-3 (CC3) antibody (Top Row). Cells in later stages of apoptosis are labeled with a PS-binding dye, PSVue (Middle Row). Overlay of CC3 (cyan) and PSVue (red) (Bottom Row). In PBS-injected controls, there is a low level of apoptotic cell death, which is concentrated in cortical layers II and IV. In EtOH-injected mice, there is an increase in both early (CC3+) and later-stage (PSVue+) apoptotic cells by 12 h. Later stage (PSVue+) apoptotic cells continue to increase at 24 h, but few apoptotic cells are evident by 48 h and after (C, EtOH). Images are Z projections of confocal image stacks spanning 54 μm. (**D**) The boxed region shows the area in which CC3 and PSVue particle analyses were performed (E and G). (**E**) Particle analysis of CC3+ structures in cortical layer IV. Error bars represent SDP (N=4-6 cortical slices). *p = 0.0004. **F**) Western blot of CC3 protein in whole cortex following PBS (--) or EtOH (+) injection. β-tubulin was the internal loading control. Timeline of caspase activation in whole cortex is in agreement with the

immunohistochemical results shown in C. (**G**) Particle analysis of PSVue+ structures in cortical layer IV. Same tissues used for analysis as in (E). *p = 0.05, **p = 0.009.

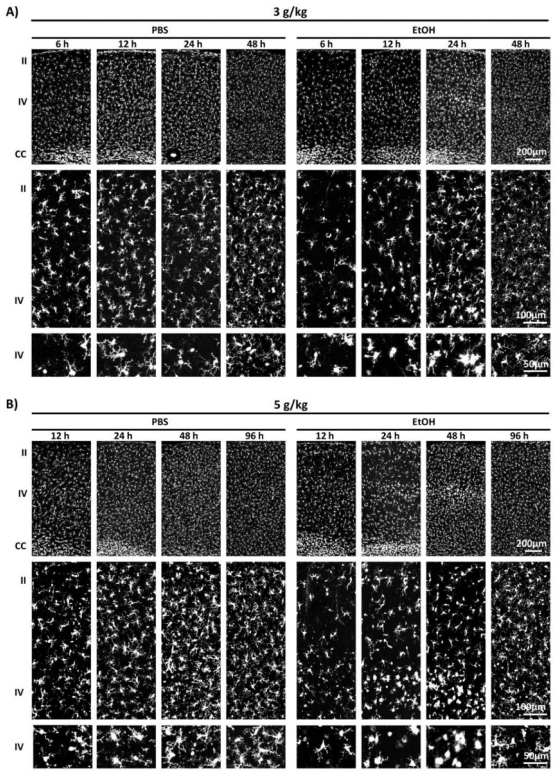

Figure 3. Acute ethanol exposure induces transient changes in the morphology and distribution of cortical microglia

Images show GFP-expressing microglia in somatosensory cortex of CX3CR1$^{GFP/+}$ mice following injection of PBS (Left) or EtOH (Right). Note differences in time-points in A and B. (**A**, 3 g/kg, Top and Middle Rows) Microglial density appears to increase from 6 to 48 h in control mice. Despite this increase in density, microglia maintain an even distribution across the cortical layers, although there are many activated microglia in the corpus callosum (CC, PBS). In contrast, following EtOH-injection, microglial density appears to increase in cortical layers II and IV from 6 to 24 h while microglial density appeared to decrease in the adjacent layers. Microglia redistribute after 24 h (EtOH). (Bottom Row) High magnification images in cortical layer IV demonstrate that microglia remain ramified following a control, PBS injection. However, over the first 24 h following EtOH injection, microglia assume a more amoeboid form. Microglial re-ramification occurs after 24 h. Images are Z projections of confocal image stacks spanning 145 µm (Top Row) and 68 µm (Middle and Bottom Rows). (**B**, 5 g/kg) Microglial changes are similar to what was seen following 3 g/kg EtOH, with the exceptions that: 1) Microglial density in cortical layers II and IV is increased for a prolonged period of time (12-48 h, Top and Middle Rows) and 2) Microglia morphological changes are more pronounced and are present from 12-48 h. Re-ramification occurs from 48-96 h following 5 g/kg EtOH exposure (Bottom Row).

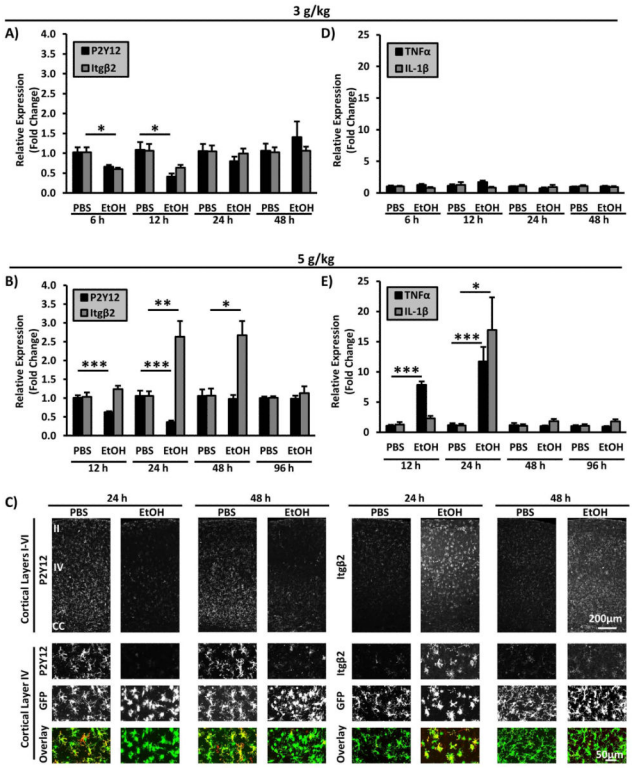

Figure 4. Acute ethanol exposure induces transient changes in molecular indicators of microglial activation

(**A**) RT-qPCR analysis of the normalized expression of molecular indicators of microglial activation in whole cortical tissues derived from 3 g/kg PBS- or EtOH-injected mice. Cortical expression of P2Y12 is decreased significantly at 12 h, but returned to control levels by 24 h. In contrast, Itgβ2 expression decreased significantly by 6 h and began to return to control levels by 12 h. (**B**) RT-qPCR analysis following 5 g/kg PBS- or EtOH injection. P2Y12 expression is decreased significantly at 12 and 24 h, but returned to control levels at 48 h. Itgβ2 expression was significantly increased at 24 and 48 h and returned to control levels by 96 h. These changes are consistent with transient microglial activation. (**C**) Low magnification images (Top Row) of the full depth of the neocortex stained for two microglial proteins, P2Y12 (Left) and Itgβ2 (Right). P2Y12 protein is decreased at 24 and 48 h following 5 g/kg EtOH-injection relative to PBS-injected controls. In contrast, Itgβ2 expression is increased at 24 and 48 h following 5 g/kg EtOH-injection relative to PBS-injected controls. Higher magnification images (Bottom Rows) of cortical layer IV demonstrate that P2Y12 and Itgβ2 expression is localized to GFP+ microglia. Images are Z-projections of confocal image stacks spanning 145 μm (Top Row) and 68 μm (Bottom Rows). (**D**) RT-qPCR analysis of the normalized expression of PIFs, TNFα and IL-1β, in whole cortical tissues derived from 3g/kg PBS- or EtOH-injected mice [same animals that were used for (A)]. There were no significant changes in expression of either TNFα or IL-1β following 3g/kg EtOH. (**E**) RT-qPCR analysis of the normalized expression of TNFα and IL-1β in whole cortical tissues derived from mice injected with 5 g/kg PBS- or EtOH [same animals that were used for (B)]. Cortical expression of TNFα and IL-1β increased significantly during the first 24 h following EtOH and then returned to control levels by 48 h

post-EtOH. Error bars represent SEM *p ≤ 0.05, **p ≤ 0.01, ***p ≤ 0.005. (N=5-8 mice per condition).

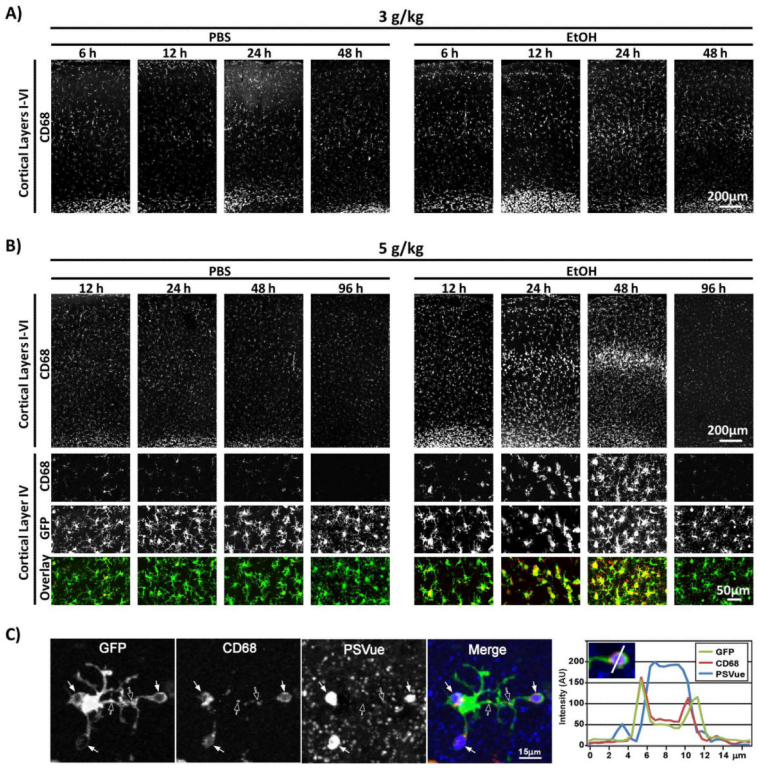

Figure 5. Acute ethanol exposure induces a transient increase in microglial lysosomal protein, macrosialin/CD68, indicative of phagocytic activity

(**A**, 3 g/kg) In PBS controls there is a low basal level of CD68 IR in cortical layers I to VI, presumably in response to a persistent level of developmental apoptosis. After EtOH-injection, CD68 IR increased especially in cortical layers II and IV from 6 to 24 h, but returned to levels comparable to PBS control by 48 h after injection. (**B**, 5 g/kg) CD68 IR is similar to what is seen following 3 g/kg EtOH, except that there is a more pronounced up-regulation of CD68 in layer IV, and CD68 down-regulation does not occur until after 48 h. (Bottom Rows) High magnification images of cortical layer IV demonstrate that strong CD68 immunostaining localizes to activated microglia. Images are Z-projections of confocal image stacks spanning 150 μm (Cortical Layers I-VI) and 72 μm (Cortical Layer IV). (**C**) Higher resolution, multi-channel confocal imaging demonstrates that CD68 is not strictly colocalized with PSVue+ structures in phagosomes. Although it is often located near microglial phagocytic profiles (solid arrows and plot profile to right), it is also found in smaller structures, likely lysosomes, in microglial branches (open arrows).

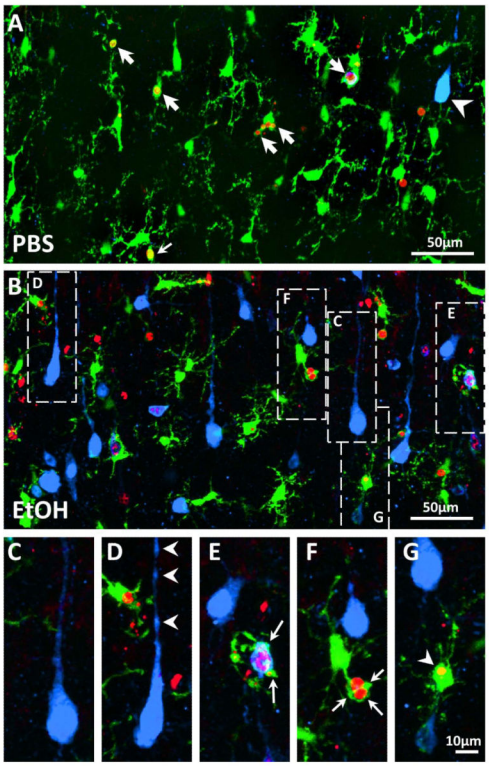

Figure 6. Microglia contact and phagocytose later stage apoptotic cells during normal development and following neonatal ethanol exposure

High magnification images of apoptotic cells (Blue and Red) and microglia (Green) in cortical layer IV, 4 h after injection of PBS (A) or 5 g/kg EtOH (B). All images are Z-projections of confocal image stacks spanning 67 μm. (**A**) Under control conditions, microglia rarely contacted CC3+ cells (Blue; Arrowhead) but often contacted or engulfed PSVue+ structures (Red; Arrows). (**B**) Similar contacts are seen following EtOH injection, with the exceptions that there is a significantly higher density of CC3+ and PSVue+ structures, and many more PSVue+ structures are not contacted by or contained within microglia. (**C-G**) Images from B arranged to indicate a possible sequence of apoptotic cell progression from early (C) to late (G) stages of apoptosis, based on size, morphology, and intensity of stained particles. (**C**) Intact-looking early apoptotic pyramidal neurons with smoothly tapering apical dendrites stain intensely for CC3. (**D**) CC3-stained neurons begin to bleb and fragment (arrowheads) as the apoptotic cascade continues. (**E**) PSVue staining begins to appear along with CC3 and intensifies as CC3 diminishes. Microglia first contact dying cells at this stage (arrows). (**F**) Compact, intense PSVue+ profiles are surrounded by microglial processes (arrows). (**G**) PSVue structures are then completely engulfed by microglia and are evident within microglial cell bodies (arrowhead).

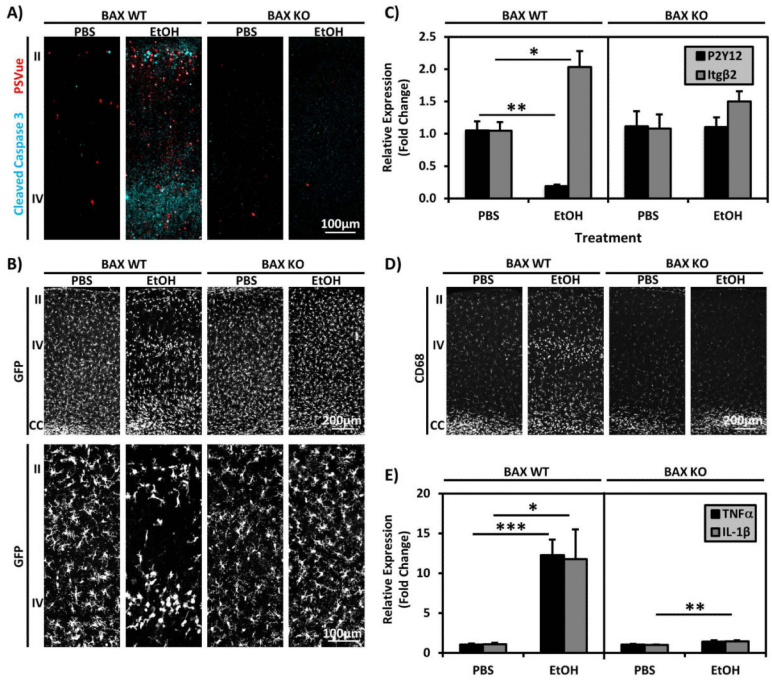

Figure 7. Microglial activation induced by acute ethanol exposure *in situ* is abrogated by BAX KO

All data in this figure were collected at 24 h after PBS or 5 g/kg EtOH injection. (**A**) Images of cortical layers II-IV show that while EtOH injection of WT mice results in a substantial increase in apoptotic cell death relative to PBS injected controls, EtOH-induced cell death is eliminated in BAX KO animals. Images are Z-projections of confocal image stacks spanning 74 μm. (**B**) Microglia in GFP-reporter:BAX WT mice respond to EtOH-induced cell death by redistributing to cortical layers II and IV (Top Row, Low Mag) and assuming an amoeboid form (Bottom Row, Higher Mag). In contrast, microglia in BAX KO mice are more evenly distributed and maintain a ramified morphology in the presence or absence of EtOH. Images are Z-projections of confocal image stacks spanning 180 μm (Top Row) and 74 μm (Bottom Row). (**C**) RT-qPCR analyses of P2Y12 and Itgβ2 mRNA in whole cortex of BAX WT animals show a molecular profile of microglial activation in response to EtOH (cf. Fig. 4B). In contrast, in BAX KO's, P2Y12 and Itgβ2 are expressed at similar levels in the presence or absence of EtOH. Error bars represent SEM. (N = 6-8 mice per condition). *p = 0.006 and **p = 0.0001. (**D**) EtOH-induced increase in CD68 IR is abrogated in BAX KO mice. (**E**) RT-qPCR analyses of mRNA in whole cortex shows that the EtOH-induced increase in TNFα and IL-1β is largely abrogated in BAX KO mice, although a minor but statistically significant increase is observed for IL-1β. (N = 6 mice per condition). *p = 0.02, **p = 0.01, *** p = 0.0002.

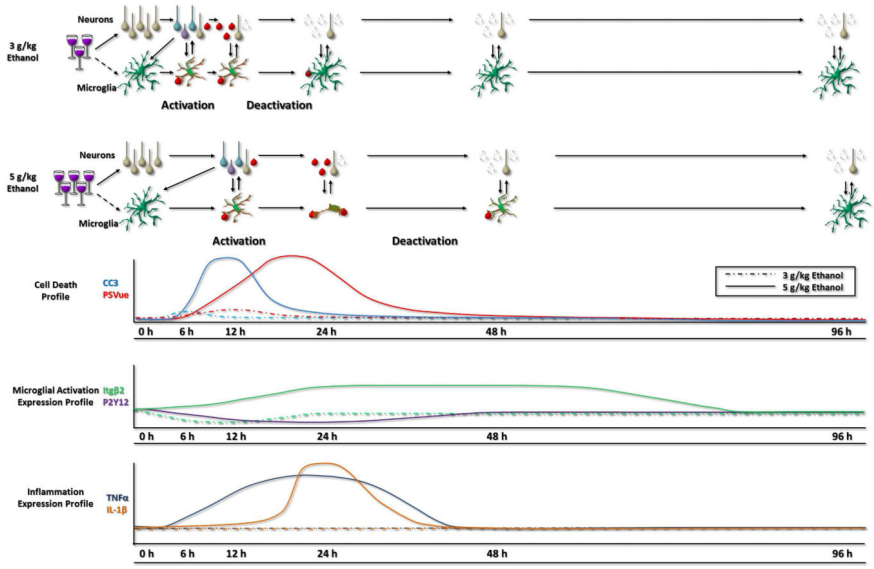

Figure 8. Graphical summary showing the relative timing of neuronal injury, microglial activation/deactivation, clearance of dead cells, and inflammatory factor expression following acute developmental alcohol exposure in situ

(**Neurons**) Exposure to 3 or 5g/kg EtOH on P7 results in significant cortical neuronal loss. As neurons begin to die, they initially activate caspase 3 (blue cells), but as cell death progresses PSVue labeling becomes more prevalent [cells transition from purple (CC3 + PSVue) to red (PSVue only)]. As these molecular transitions underlying cell death occur, the neurons condense into increasingly more compact structures. (**Cell Death Profile**) Time-line for the appearance of CC3 and PSVue, indicators of early and later stages of apoptosis, respectively. Note, the level of cell death scales with the BAC (Dashed Lines – 3 g/kg EtOH, Solid Lines – 5 g/kg EtOH). (**Microglia, Activation**) Analysis of BAX KO mice indicates that acute EtOH exposure has little direct effect on microglial activation in neonatal mice *in situ* (dashed arrow). However, in direct response to the EtOH-induced apoptotic cell death (solid arrows), microglia undergo morphological (**Change in Cell Shape**) and molecular (red hue) changes associated with activation (**Microglial Activation Expression Profile**) that scale with the insult. Activated microglia up-regulate the expression of a lysosomal protein, CD68, and begin to phagocytose PSVue+ dead cells. Phagocytic clearance is depicted as microglia processes physically surrounding PSVue+ cells (red), and in the cell's subsequent removal from the tissue. (**Microglia, Deactivation**) Once apoptotic cells are removed from the cortex, microglia deactivate. During this time, microglia re-ramify, down-regulate CD68, and other molecular correlates of activation return to baseline. (**Inflammation Expression Profile**) Expression of PIFs TNFα and IL-1β increase coincident with microglial activation following 5 g/kg alcohol exposure and quickly return to baseline as dead cells are cleared and microglia deactivate.